Scanner characterization for color measurement and diagnostics

Bong-Sun Lee
Thomson Corporate Research
2233 North Ontario Street, Suite 100
Burbank, California 91504

Raja Bala
Xerox Research Center Webster
800 Phillips Road, Building 128-27E
Webster, New York 14580

Gaurav Sharma
University of Rochester
Electrical and Computer Engineering Department and
Department of Biostatistics and Computational Biology
Hopeman 204, RC Box 270126
Rochester, New York 14627-0126

Abstract. *We propose a novel scanner characterization approach for applications requiring color measurement of hardcopy output in calibration, characterization, and diagnostics applications. The method is advantageous for common practical color printing systems that use more than the minimum of three colorants necessary for subtractive color reproduction; printing with cyan (C), magenta (M), yellow (Y), and black (K) is the most prevalent example we use in our description. The proposed method exploits the fact that for the scenarios in consideration, in addition to the scanner RGB values for a scanned patch, the CMYK control values used to print the patch are also available and can be exploited in characterization. An indexed family of 3D scanner characterizations is created, each characterization providing a mapping from scanner RGB to CIELAB for a fixed value of K, the latter constituting the index for the characterization. Combined together, the family of 3D characterizations provides a single 4D characterization that maps scanner RGB obtained from scanning a patch and the K control value used for printing the patch to a colorimetric CIELAB measurement for the patch. A significant improvement in the robustness of the method to variations in printing is obtained by modifying the K index to utilize the scanned output for a black-only patch printed with the corresponding K value instead of directly utilizing the control K value used at the printer. Results show that the proposed 4D scanner characterization technique can significantly outperform standard 3D approaches in the target applications.* © *2007 SPIE and IS&T.*
[DOI: 10.1117/1.2803833]

1 Introduction

Color measurement is an essential function in any color management system and is required in order to perform tasks such as device calibration, characterization, quality evaluation, and diagnostics. Colorimeters and spectrophotometers are the primary devices used for the purpose of color measurement. While these devices offer excellent accuracy and precision, they are typically expensive and require skilled operators.

On the other hand, color scanners with improved functionality and quality are becoming increasingly cheaper and are now commonly available. It would be beneficial if such scanners could be used as an inexpensive alternative for colorimetric measurement of hardcopy prints. As an added advantage, the high spatial resolution offered by most modern scanners enables one to measure the spatial variations in prints, in addition to the average color.[1–3] The main barrier to using scanners for color measurement is that their response is typically not colorimetric, i.e., it is not identical to, or even linearly related to, that of the human visual system. Methods exist to characterize and correct scanners for this shortfall; however, they have certain fundamental limitations, as described next.

The device (usually RGB) signals acquired from a scanner are related to a spectral or colorimetric representation through the process of scanner characterization. Standard approaches create a scanner characterization profile by scanning a printed target containing a set of color patches. The target is simultaneously measured with a color measurement device to obtain spectral reflectance or colorimetric measurements such as CIELAB. The scanned RGB and corresponding colorimetric data are related via a 3D transform (such as a 3×3 matrix, polynomial, etc.). Figure 1 shows such a scanner characterization process. This procedure must generally be repeated for each input medium (i.e., combination of substrate, colorants, and image path elements). Thus, for example, different scanner color char-

Paper 06124R received Jul. 13, 2006; revised manuscript received Mar. 19, 2007; accepted for publication Jun. 15, 2007; published online Nov. 8, 2007. Parts of this work were presented at the SPIE conference on Computational Imaging IV, Jan. 2006, San Jose, Calif. and were published (unrefereed) in SPIE Proceedings Vol. 6065.
1017-9909/2007/16(4)/043009/13/$25.00 © 2007 SPIE and IS&T.

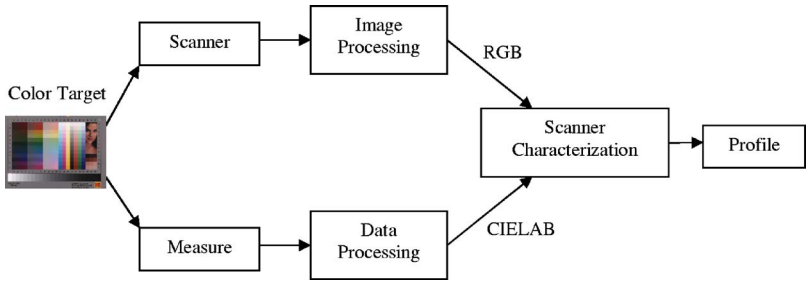

Fig. 1 Standard scanner characterization.

acterization profiles are required for use with a photograph and a xerographically produced print. The primary reason for this is that, as stated earlier, color scanners are generally not colorimetric,[4–7] so that the relationship between the response of the scanner and that of the human eye is nonlinear and dependent upon the spectral properties of the medium being scanned. Thus, scanner characterization relies on the limited degrees of freedom exploited in the input medium rather than on the limited spectral sampling in the human visual system.[8,9]

Due to the noncolorimetric characteristics mentioned in the preceding paragraph, an important consideration in scanner characterization is the choice of colorants used to make the printed colors. The basic subtractive primaries in printing are cyan (C), magenta (M), and yellow (Y). However, many marking processes, e.g., lithography, xerography, and inkjet, use additional colorants for reasons of economy and for expanding the reproducible gamut. The most common example, and the one used to illustrate our new approach, is black (K). Other examples include "hifidelity" colorants such as orange and green. Whenever four or more colorants are used, there is an inherent redundancy in that different colorant combinations can result in the same 3-dimensional response from either the human eye or the scanner. Thus, the scanner characterization function depends not only on the physical properties of the medium, but also on the particular colorant combinations being scanned. Experiments have demonstrated that even for a single printer, the scanner characterization shows significant dependence on the strategy used to combine the CMYK colorants via undercolor removal (UCR) and gray component replacement (GCR).[8]

Standard approaches to scanner characterization for 4 or more printed colorants make fixed *a priori* assumptions about the colorant combinations. As an example, targets from CMYK lithographic or xerographic processes are defined colorimetrically[10] and then printed using a predetermined suitable UCR/GCR strategy, which constrains the amount of K used with a given CMY combination. This approach is justified by the assumption that the lithographic pictorial images that one expects to scan in the final application are also subject to the same or similar UCR/GCR constraint.

A problem arises when CMYK images are encountered that deviate from the assumed UCR/GCR strategy. For example, the CMYK values used to create test images for printer defect identification are not necessarily subject to the UCR/GCR constraints normally used for pictorial images. Thus, the use of a scanner characterization optimized for a fixed UCR/GCR strategy may give erroneous results. Another application where it may be desirable to use the scanner as a color measurement device is printer calibration and characterization. These tasks involve printing and measuring targets comprising patches of various (preferably unconstrained) CMYK combinations, and modeling the printer's response throughout its gamut. In this application one cannot generally assume that the target being scanned has been generated with any fixed UCR/GCR strategy. Thus, a standard scanner characterization designed for capturing pictorial images generated with a standard UCR/GCR would not be "trained" to accurately measure all the patches for printer calibration and characterization.

For the reasons outlined above, conventional scanner characterization methods often do not provide enough accuracy in order to allow use of a scanner as a color measurement device for printer calibration, characterization, or diagnostics applications. In this paper, we propose an alternative scanner characterization method for these applications. The proposed method exploits auxiliary information that is available in the color scanning for diagnostics and calibration scenarios, i.e., the colorant values that are used to generate the printed targets. Using this auxiliary information along with suitable target design, our method effectively reduces the degrees of freedom in the input that are "seen" by the scanner characterization. Matching the effective degrees of freedom addressed by the scanner characterization to the three degrees of freedom that can be captured by the three scanner channels results in significant improvement in accuracy (for these applications).

2 Scanner Characterization for Known Colorant Values

We propose a novel scanner characterization approach that is intended especially for printer calibration, characterization, and diagnostics applications where the scanner is used to measure printed color patches generated by four or more colorants and where the digital colorant amounts being sent to the printer are known. We will use the example of CMYK colorants to describe the method. Generalization to other additional colorants using the same underlying principles is straightforward.

2.1 *Conceptual Foundation*

As stated previously, standard scanner characterization is a mapping from scanner RGB to device-independent color coordinates such as CIELAB. Since the spectral reflectance of a CMYK print depends on four independent

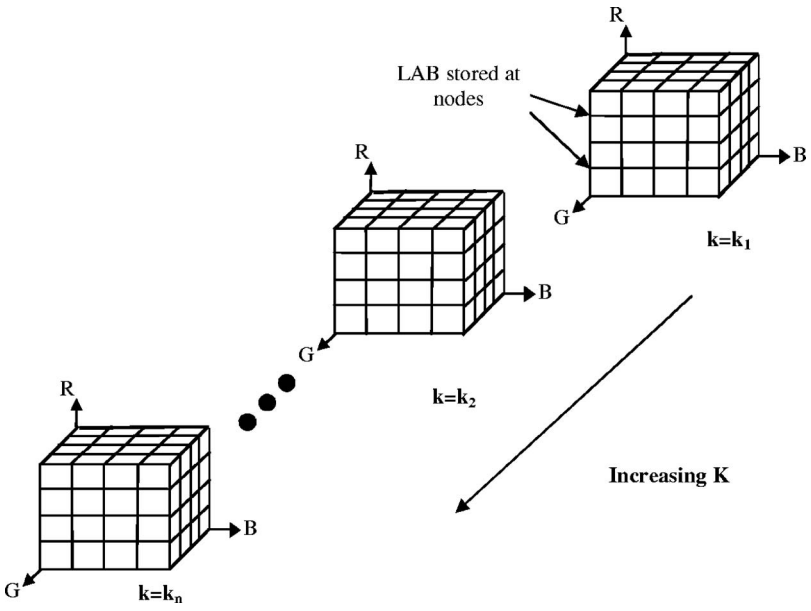

Fig. 2 Family of 3D scanner characterization LUTs mapping scan RGB to CIELAB for different levels of K.

parameters—i.e., the C, M, Y, K control values—one can expect to obtain an accurate scanner characterization (despite the fact that the scanner is noncolorimetric) if the scanned values capture these four independent parameters. Thus, it is logical to expect that the scanner characterization is also a function of four (rather than three) variables. In our proposed approach, we capture the dependence explicitly by introducing a fourth input dimension in addition to the usual dimensions of a scanner, R, G, B. The additional dimension is related to the amount of K present in the print, so we begin by assuming that the fourth dimension corresponds to the digital control value of K. This is later refined in order to account for variability in printing due to which the printed amount of black colorant, which is in fact the determinant of the colorimetry, can vary for the same digital control value of the K channel.

It is helpful to think of the 4-dimensional scanner characterization transform as a family of 3D scanner characterizations, each derived for a fixed digital level of K using standard methods. This is accomplished by printing, for each level of K, a target comprising a 3D grid varying in C, M, and Y. The patches are measured in CIELAB as well as scanned in RGB. For each fixed level of K, any standard technique such as neural network optimization or polynomial regression[11] can be used to derive a scanner characterization transform that maps scan RGB to CIELAB with high accuracy. In order to afford efficient processing of image data through the characterization transform, the latter is usually implemented as a 3D lookup table (LUT) mapping scan RGB to CIELAB. The result is therefore a family of 3D LUTs each corresponding to a fixed level of K, as shown in Fig. 2. The levels of K can be selected to optimize the overall characterization accuracy.

In a second step, the family of 3D LUTs is combined into a single 4D LUT mapping KRGB to CIELAB. This allows determination of the scanner characterization transform for arbitrary levels of K in the image via interpolation among the precharacterized K levels.

2.2 *Target Design*

The layout of the scanner characterization target comprises blocks of $C \times M \times Y$ grids at each fixed level of K and is graphically illustrated in Fig. 3. The spatial arrangement has been chosen such that similar colors are adjacent to each other. This arrangement is intended to minimize the integrating cavity effect (ICE)[12,13] frequently encountered in desktop scanners. Preferrably, the patches at the edges of the target are replicated to form an extra border of "dummy

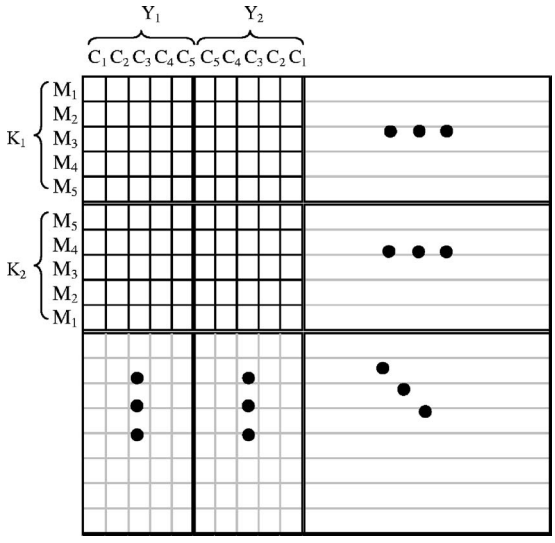

Fig. 3 Layout of the 4D target.

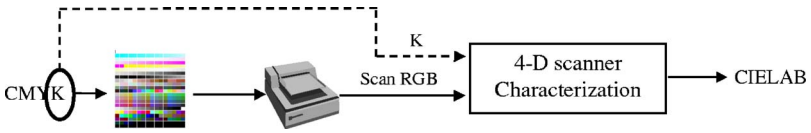

Fig. 4 Application of 4D scanner characterization for color measurement.

patches." This is done again to minimize ICE, which is most pronounced when color patches are adjacent to a white background. The indexing notation is such that C_1 is the least amount of cyan, C_5 is the largest amount of cyan, etc. The levels along each colorant axis, C_i, M_j, and Y_k, can be chosen in a number of ways. In our experiments they were chosen to be approximately visually uniform by processing evenly spaced digital values through calibration curves derived for the printer at a previous time.

2.3 *Application of the Scanner Characterization Transform*

Figure 4 shows the final application of 4D scanner characterization for color measurement. A test target (e.g., printer diagnostics or calibration target) is scanned, and the scanned RGB values and the associated K are indexed into a 4D LUT. The output of this LUT are the CIELAB values of the test target. There are several methods of obtaining the K amount associated with each scanned RGB pixel. If the image is a patch target, a simple approach is to retrieve the K value used in each patch from a database associated with the target. A more general but difficult approach would be to estimate the K amount directly from analysis of the scan of each patch.[14]

2.4 *Accounting for Printer Variability*

Thus far, in our description, the fourth dimension in the scanner characterization has been assumed to be the digital K value used to generate the printed color. A limitation of this approach is that the true scanner response depends on the actual printed amount of black, rather than the digital control value of K for the patch; and the relationship between digital K channel control value and actual printed amount of black colorant can vary from device to device and over time. This variation can thus potentially reduce the accuracy of a scanner characterization indexed by digital K values. To overcome this limitation, it is preferable to use an estimate of the actual printed K rather than the digital K value as the fourth dimension in the scanner characterization. To this end, we propose using the scanner's green response to pure K prints as the fourth dimension in the scanner characterization's LUT. The green channel is used since it is a rough approximation of luminance and exhibits good dynamic range in response to printed K. We will denote this fourth dimension as G_k. As will be seen in the results, G_k effectively captures variations in the printer's black response.

To derive G_k as a function of digital K, recall that the scanner characterization target is a family of CMY grids, each grid made at a fixed level of K. In the proposed method, a pure K stepwedge is included in the target. The stepwedge comprises those levels of K used to create the CMY grids. The scanner's green response to this stepwedge provides a 1D function mapping digital K to G_k. The latter is then used to index into the respective 3D characterization from scan RGB to CIELAB. The final transform is a 4D LUT mapping G_kRGB to CIELAB.

In the final application, the printed target being scanned can be specially designed so that every CMYK patch associated with it has a corresponding patch with the same amount of K, and $C=M=Y=0$. The software that parses the scanned RGB file must retrieve for each CMYK patch the corresponding pure K patch on the target. The scanned RGB for the CMYK patch and the scanned G_k for the pure K patch are then fed into the 4D characterization LUT to obtain the CIELAB representation for the CMYK patch. One way to facilitate the correspondence between CMYK and pure K patches is to use a special target layout whereby, for example, each row of patches is made of the same K value, and the first patch in the row is made of pure K. This approach offers an additional advantage that one no longer has to keep separate track of the digital K values used in the characterization and in the scans for the characterization, making the entire process less error-prone.

The point to be emphasized is that since the fourth dimension to the scanner characterization is now a scanned attribute of actual printed K rather than input digital K value, the technique is "self-calibrating" and mitigates the effect of variations in printed K over time and across devices. As a result, a single scanner characterization derived from a target generated by one printer at one given time enables the scanner to be used as an accurate color measurement for multiple printers (preferably within the same family) over a considerable period of time. This makes the approach a powerful technique for calibration and characterization of fleets of printing devices. As mentioned earlier, this does require the inclusion of patches of pure K, not only during the derivation of the scanner characterization, but also during the application of the scanner characterization for color measurement.

3 Experiments

A Xerox DocuColor-12 CMYK laser printer and two desktop scanners, a Umax and an Epson, were used for the experiments. All colorimetric measurements were taken with a Gretag SpectroLino spectrophotometer mounted on a SpectroScan stage.

Three scanner characterization techniques were compared: (1) standard 3D approach; (2) Monaco EZColor, a popular scanner profiling package that builds a standard 3D ICC profile; and (3) the proposed 4D approach. Each of these is described next.

3.1 *Implementation of 3D Scanner Characterization*

3.1.1 *Standard approach*

A standard IT8.7/2 target comprising 288 patches was printed on a DocuColor 12 printer. This target was mea-

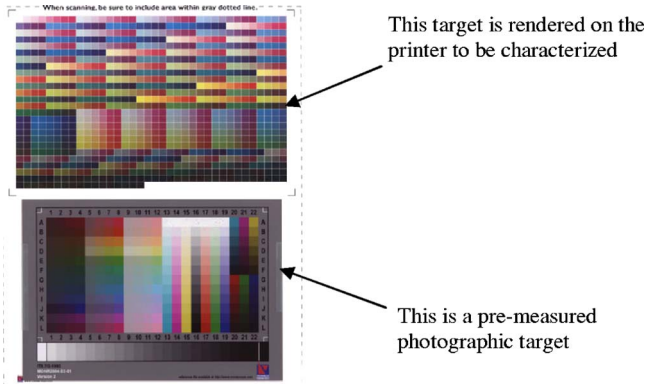

Fig. 5 Test target used by Monaco EZcolor package.

sured using the Gretag SpectroLino to obtain CIELAB values. D50 was chosen as the illuminant, and all color calculations were based on media-relative colorimetry (i.e., white paper was set to $L^*:100$, $a^*:0$, $b^*:0$). The target was scanned on the Umax scanner with settings of 300-dpi resolution and tone correction $\gamma=1.0$. All automatic adjustments in the scanner software were turned off. On the Epson scanner, the same target was scanned at 300 dpi and $\gamma=1.6$ (chosen to avoid clipping artifacts). The scanned image was mapped through the inverse gamma function to produce an image with $\gamma=1.0$. Floating-point precision was used for the gamma conversions. To minimize the effects of scanner nonuniformity, we scanned the same target with two different orientations and used the average scan for the characterization.

For each patch in the IT8 target, the average of a window of pixels within each patch was computed. The window size was 70% of the patch size in each dimension (this produced an acceptable signal-to-noise ratio). Using the scan RGB and corresponding CIELAB measurements of the IT8 target, a 3D LUT mapping RGB to CIELAB was derived. For the LUT derivation, we chose a neural network approach using a procedure similar to that described in Ref. 11. The size of the LUT was $16\times16\times16$.

3.1.2 *Monaco EZcolor*

This profiling tool characterizes and creates ICC profiles for input and output devices. The user prints a characterization target on the printer he wishes to characterize. He then attaches a premeasured photographic IT8 scanner characterization target to this print, as shown in Fig. 5. This composite target is scanned, and two ICC profiles are generated, one for the scanner and one for the printer. We used this procedure to generate profiles for the Umax and Epson scanners as well as the DocuColor 12 printer. Note that the scanner profiles are derived from a generic photographic target.

3.2 *Implementation of 4D Scanner Characterization*

The 4D characterization target was constructed as explained in Section 2.2. The target consisted of six blocks of patches consisting of a CMY grid at different levels of K: $K_1=0$, $K_6=255$. In addition, a series of C, M, Y, and K stepwedges was included to generate a tone reproduction curve (TRC) for each colorant. Specifically, the K stepwedge was used to derive the transformation from K to G_k, and included the six levels of K corresponding to the CMY grids. The specific levels in the K stepwedge were chosen to be approximately visually uniform by processing an evenly spaced set of digital K values through a previously derived printer calibration TRC that linearized the K channel to visual ΔE from paper. The number of different levels of K required was experimentally determined. An initial test with 5 levels produced large characterization errors especially for pure K patches. This is depicted in Fig. 6(a). The plot shows the characterization (prediction) errors for a step wedge of 25 pure K levels ranging from 0–255. To account for possible spatial nonuniformity in the printer, two stepwedges were used—one in increasing order of K, viz. light to dark, and the other in decreasing order, i.e., dark to light. Note that in Fig. 6(a) the errors are low when the value of K coincides with one of the five chosen levels for the black $K_1,\ldots,K_5$, and high for intermediate levels of K. As shown in Fig. 6(b), adding 5 more levels of K at the intermediate values that gave the large errors reduced the errors significantly. Since space limitations on the page prevent the use of all 10 levels, we chose the six best combinations of K levels that yielded a minimal ΔE. As a result, we obtained a substantial improvement, as shown in Fig. 6(c). These 6 levels were used in the 4D target. The digital values for those six levels were [0, 43, 96, 117, 160, 255].

As the K level increases, the patches obviously get

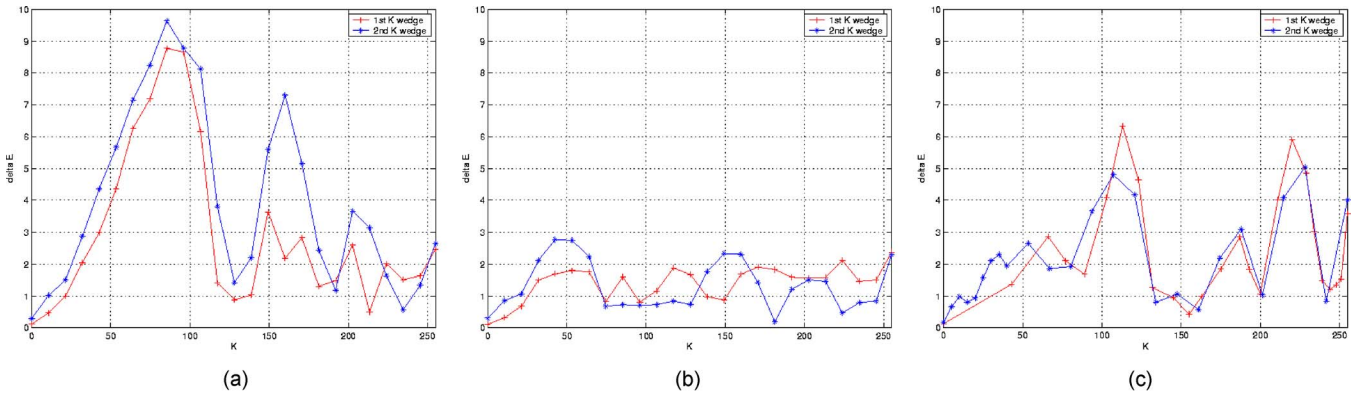

Fig. 6 ΔE for two pure K wedges in the 4D target. (a) 5 K levels; (b) 10 K levels; (c) 6 K levels selected.

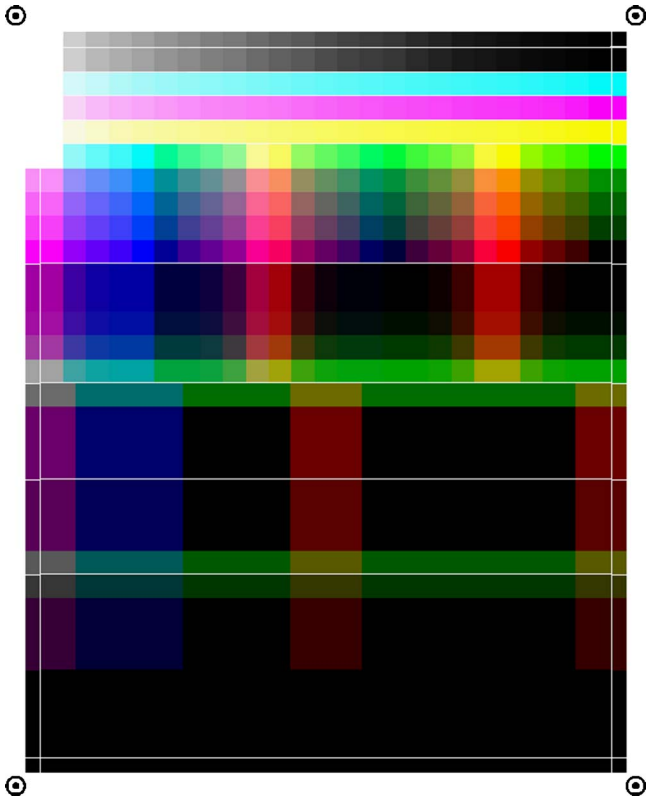

Fig. 7 Characterization target for 4D approach [the target layout is best seen in the electronic (color) version of this figure].

darker, therefore becoming more susceptible to noise in the scanning process. To mitigate this effect, the size of the darker patches is increased, and a larger averaging window is used within the scanned image. Also, patches in the last block at $K=K_6$ are all duplicated. This enabled two spectrophotometric measurements per color, thus further reducing the effect of noise.

The 4D scanner target described in Section 2.2 and shown in Fig. 7 was generated and printed on the DocuColor 12 printer. The target was measured and scanned with the same procedure as with the 3D case. A TRC was constructed that mapped digital K to G_k, the scanner's response to pure K. Figure 8 shows plots of G_k vs. K for the Umax and Epson scanners. Note that Figs. 8(a) and 8(b) both exhibit the same basic shape and approach saturation toward the highlight (low-K) region. The Umax response appears to exhibit some clipping in the highlight region. We suspect that this effect and other minor differences between the two scanner responses are largely due to experimental variation. (Gamma correction was not applied to the Umax scanner, because we never observed systematic clipping effects in pilot experiments.)

Next we derived the 4D LUT. We first derived six 3D LUTs, one for each of the six blocks $B_1, \ldots, B_6$ as shown in Fig. 9. These six LUTs mapped scanned RGB to CIELAB, each LUT corresponding to a different constant value of K. The scanner's green response G_k to each of the six pure K patches was extracted from the K wedge in the target to obtain the fourth scanner dimension. These six 3D LUTs were then combined into a single 4D LUT that would map scanned G_kRGB to CIELAB. The LUT size was $6\times16\times16\times16$. Note that six LUTs were concatenated in reverse order so that the LUT for the highest K level positioned first in the 4-D LUT and the LUT for the least K level located last in the 4D LUT. The fourth dimension G_k was also ordered correspondingly. This was done to optimize the tetrahedral interpolation.

3.3 *Evaluation Methodology*

3.3.1 *Evaluation of scanner characterization*

We used an independent CMYK test target (called "CMYK336") to evaluate the performance of each scanner characterization approach. This target consisted of 336 CMYK patches distributed throughout the printer's gamut. The target was measured as well as scanned with the same

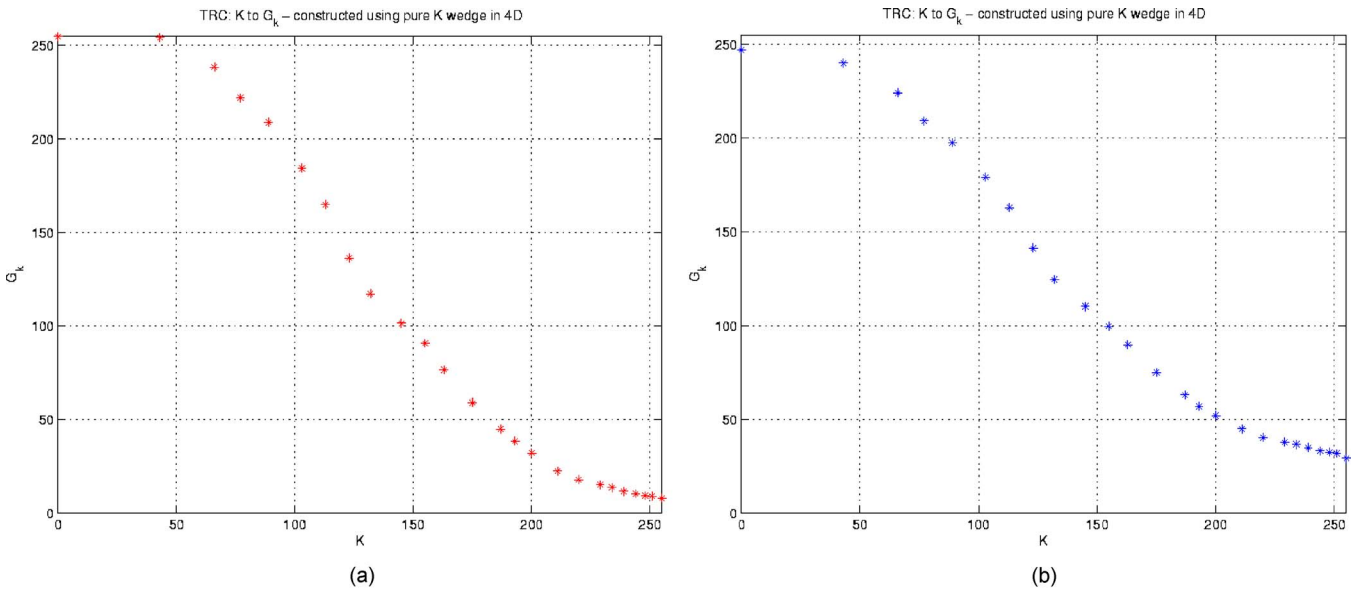

Fig. 8 Mapping from K to G_k for (a) Umax (b) Epson scanner.

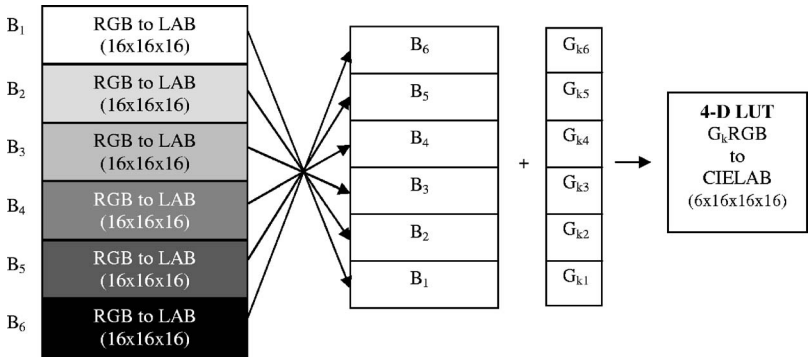

Fig. 9 Procedure for deriving 4D LUT.

settings described above. The scanned RGB data were processed through the respective scanner characterization transforms to produce CIELAB values. These were then compared with the true measurements using ΔE^*_{76} and ΔE^*_{94} metrics. Figure 10 depicts the entire test procedure for each characterization method. For the 4D approach, the G_k function was derived as a spline fit from a stepwedge of pure K patches included on the CMYK336 target.

3.3.2 *Evaluation of scanner-based characterization of the printer*

Each of the three scanner characterization techniques effectively turns the scanner into a colorimetric measurement device. This "device" can now be used to calibrate and characterize a printer. We can therefore test the efficacy of each scanner characterization technique by evaluating the quality of the resulting printer correction, as follows.

Recall from the previous procedure that we have a 336-patch target with known CMYK values and corresponding LAB values obtained from one of the aforementioned scanner characterization techniques. From this we can derive a forward printer transform from CMYK to LAB,[11] which in turn can be used to generate the inverse printer transform from LAB to CMYK. Since this is the inverse transform used in the actual color management step, we are interested in its accuracy. To this end we generate a CIELAB target comprising 240 CIELAB colors within the printer's gamut. This target is processed through the inverse transform, printed, and measured. The ΔE between the original target CIELAB and the measured CIELAB indicates the accuracy of the printer characterization. Figure 11 shows the block diagram of this application procedure. This process is repeated for each scanner characterization technique. In addition, as a baseline, we perform a similar procedure but replace the scanner characterization step with true measurements of the 336-patch target. We expect this approach to give us an upper bound on accuracy, since it replaces the scanner with spectrophotometric measurements.

3.3.3 *Consistency across scanners, halftones, and substrates*

We evaluated the robustness of a given scanner characterization technique with respect to different scanners. This was accomplished by computing ΔE between the CIELAB outputs from the given scanner characterization algorithm derived for the Epson vs. the Umax scanner.

In addition, we evaluated robustness with respect to properties of the input medium being scanned; namely, the halftone and substrate. In general, we expect that a scanner characterization produces the most accurate colorimetric

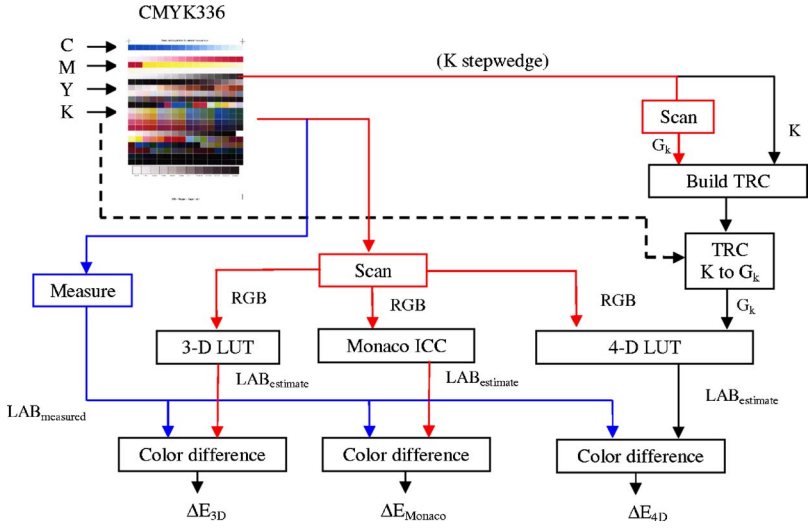

Fig. 10 Test procedure for each characterization method.

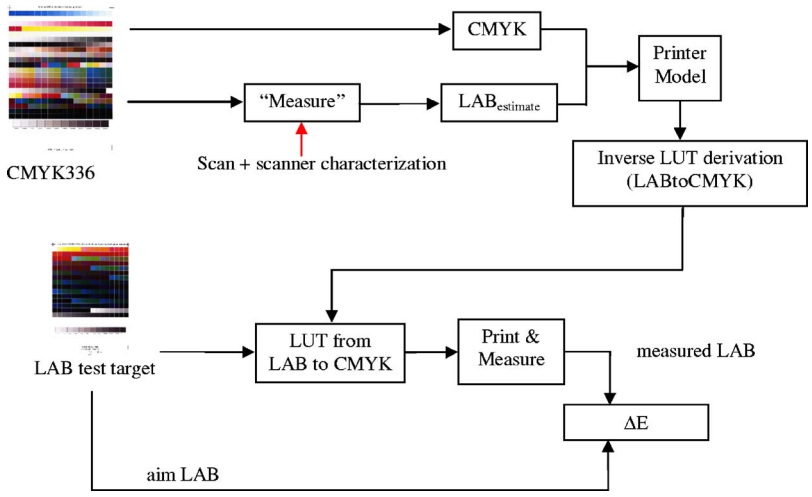

Fig. 11 Application of scanner characterization to printer color correction.

data when the substrate used in the final application is the same as that used to derive the characterization. To test robustness, we created the scanner characterization target on a bright white substrate and printed the test evaluation target on a duller matte substrate. A similar experiment was conducted to test robustness with respect to the halftoning scheme used to create the printed targets. Different halftone screens were used to create the characterization target and the test evaluation target. In both cases, all other parameters (i.e., the device and the colorants) were kept constant.

4 Results

In this section, we first present the scanner response G_k to K stepwedges and demonstrate its usefulness as a fourth dimension that accounts for print variability. Next we describe scanner characterization results with the "CMYK336" target (described in Section 3.3). We then present results for scanner-based characterization of the printer. Finally, we present results of experiments evaluating robustness across different substrates and halftones.

4.1 *Scanner Response G_k as the Fourth Dimension*

We created a K stepwedge on two different targets, printed them at different times, and measured the L^* value for each digital K level. The measurements are shown in Fig. 12(a) and reveal significant differences, suggesting that the actual printed K varied substantially across the targets. The targets were also scanned, and the green signal G_k was recorded for each patch. As seen from Fig. 12(b), the relationship between scanner G_k and L^* is largely unaffected across the two targets. This suggests that G_k correlates well with actual printed K.

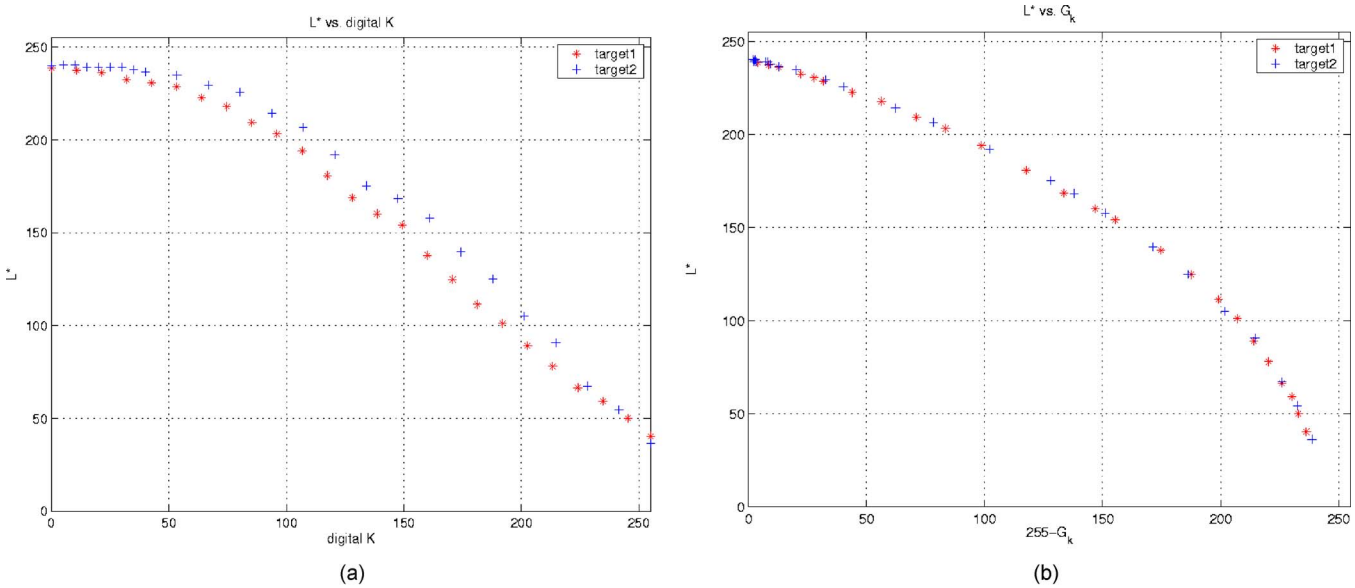

Fig. 12 Advantage of using scanner G_k rather than digital K. (a) L^* vs. digital K for a K stepwedge printed at two different times; (b) L^* vs. scanner G_k for the same two stepwedges.

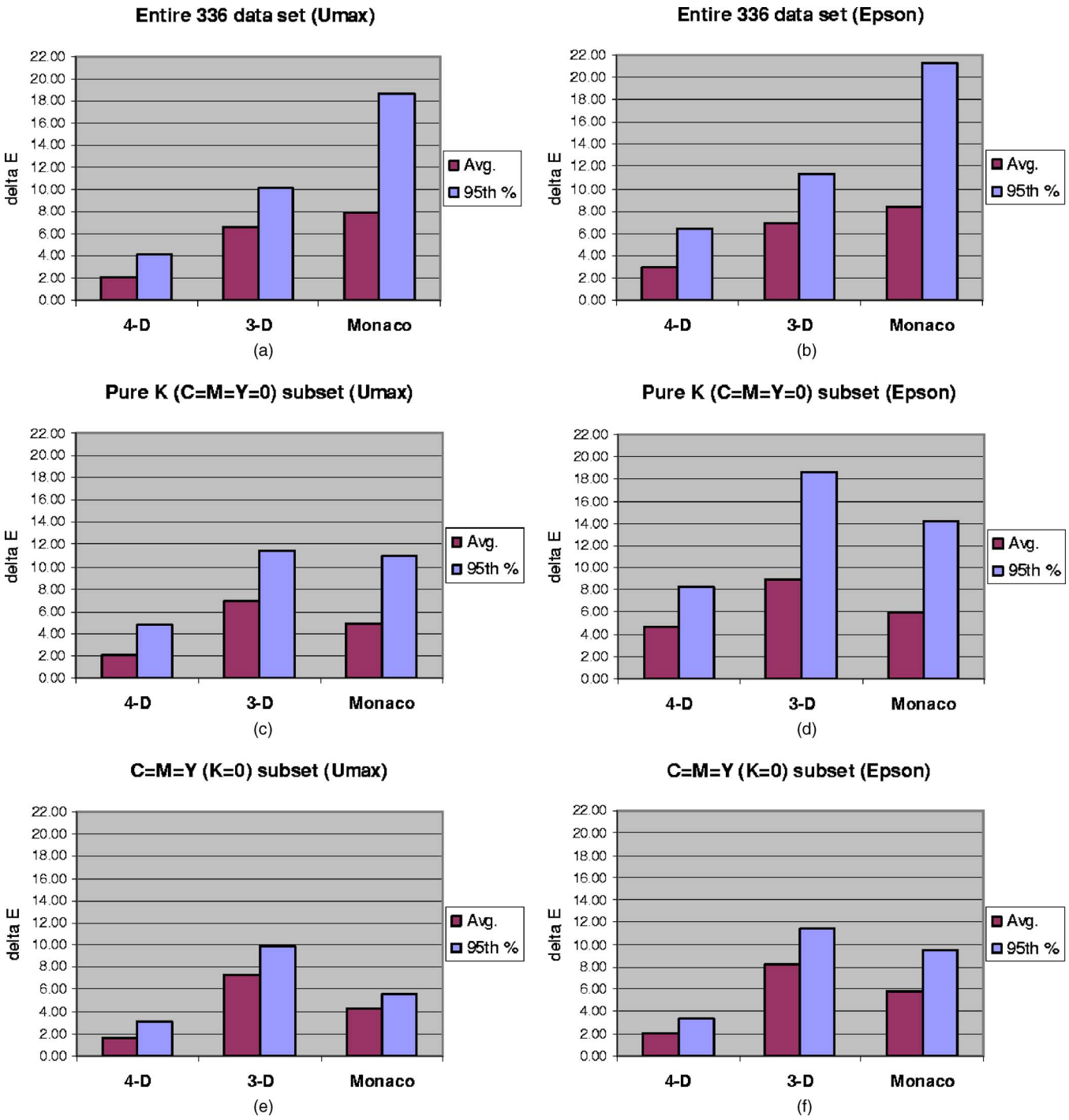

Fig. 13 Performance comparison of different approaches.

4.2 *Scanner Characterization Accuracy*

Figure 13 compares the accuracy of the 3D, Monaco, and 4D techniques. The corresponding numerical data are included in Table 1. The first two charts at the top present errors for the entire data set of 336 patches. The Monaco EZcolor technique produced the largest errors. The errors produced by the standard technique (3D approach) are also unacceptable for many applications, including printer characterization and diagnostics. The proposed technique (4D) offers a great improvement over 3D and Monaco EZcolor, as it uses a 4D characterization transform, thus allowing the dependence on the fourth dimension (K) to be explicitly captured.

Note that a fraction of these patches lies along the "upper" surfaces of the gamut for which UCR/GCR has no effect, and $K=0$. For these patches, we expect all three techniques to perform comparably. Given this fact, one can deduce that the improvement produced by the proposed technique is even greater in those regions where UCR/GCR has a strong effect. To validate this, the two plots in the

Table 1 Average color error (in CIE ΔE^*_{76} units) obtained for the different calibration methods over indicated subsets of printer patches. The proposed method corresponds to the columns labeled "4D."

		Umax			Epson		
	ΔE^*_{76}	4D	3D	Monaco	4D	3D	Monaco
Entire 336 data set	Avg.	2.09	6.59	7.87	2.90	6.85	8.45
	95th%	4.17	10.13	18.70	6.49	11.33	21.34
Pure K (C=M=Y=0)	Avg.	2.13	6.93	4.89	4.66	8.91	5.99
	95th%	4.80	11.46	10.97	8.22	18.65	14.18
C=M=Y (K=0)	Avg.	1.66	7.38	4.31	2.11	8.23	5.74
	95th%	3.14	9.92	5.54	3.35	11.44	9.45

second row of Fig. 13 present results for a subset of 25 patches containing K only (C=M=Y=0). We notice a dramatic improvement with the proposed method. The last row of figures presents analogous results for a subset of 12 patches with C=M=Y, K=0. Once again, the proposed approach is noticeably more accurate than the standard method and third-party software. The last two rows of plots also demonstrate the value of the 4D characterization method in performing printer gray-balance calibration and K linearization using a scanner as a measurement device.

It might appear at first glance that 4D characterization outperforms the 3D counterparts simply because it uses more training data, encompassing all possible CMYK combinations. Experiments wherein the same CMYK target used for the 4D technique is also used for the 3D characterization, however, demonstrate that the 4D method is still noticeably superior. The reason is that the 4D method can distinguish scanner metamers that differ in their K amounts and use different RGB-to-CIELAB transformations for these, while the 3D method is blind to the K dimension and effectively attempts to find a compromise RGB-to-CIELAB scanner characterization transformation across all the different values of K. When the universe of printed media is restricted to a 3D manifold of CMYK (as imposed by, e.g., UCR/GCR constraints), the 3D transform performs as well as the 4D one. If we generalize this notion to encompass all such manifolds by computing a separate 3D transform for each manifold, we arrive precisely at the 4D transformation.

When examining the results in Fig. 13, it is important to keep in mind the other sources of color errors in the system. LUT interpolation errors can typically produce average $\Delta E^*_{76} \approx 1.0$. Another important source of error is page-to-page variation in the printing process. In our experience, this can give rise to average ΔE^*_{76} values between 1.0 and 2.5. In light of these underlying system errors, we see in Fig. 13 that the 4D approach achieves excellent accuracy. We note finally that similar trends were observed when computing the ΔE^*_{94} metric instead of ΔE^*_{76}.

4.3 *Scanner-Based Printer Characterization*

Figure 14 compares the effectiveness of the three scanner characterization techniques in characterizing a printer. The 4D technique produces a printer model whose accuracy is equivalent to that achieved by colorimetric measurement,

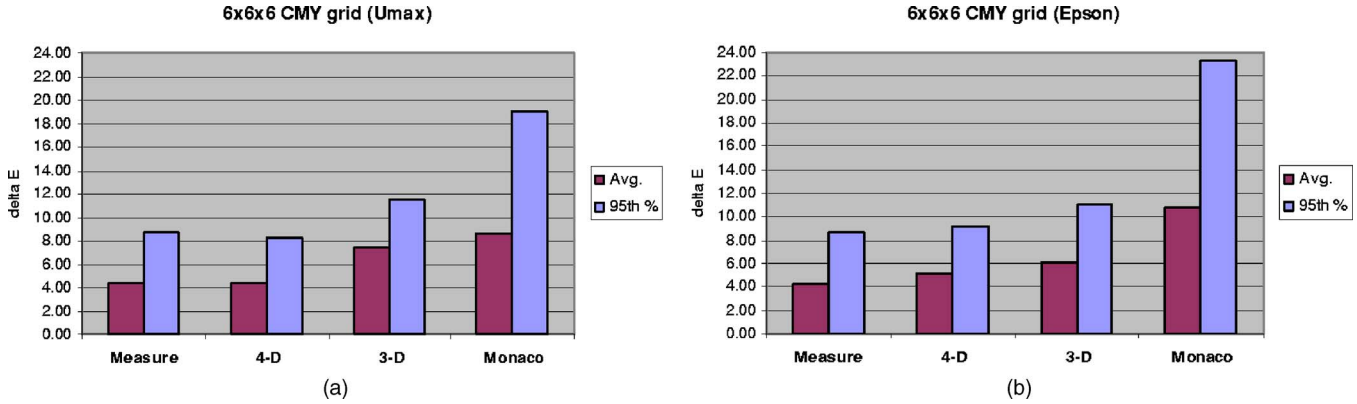

Fig. 14 End-to-end test for different characterization methods.

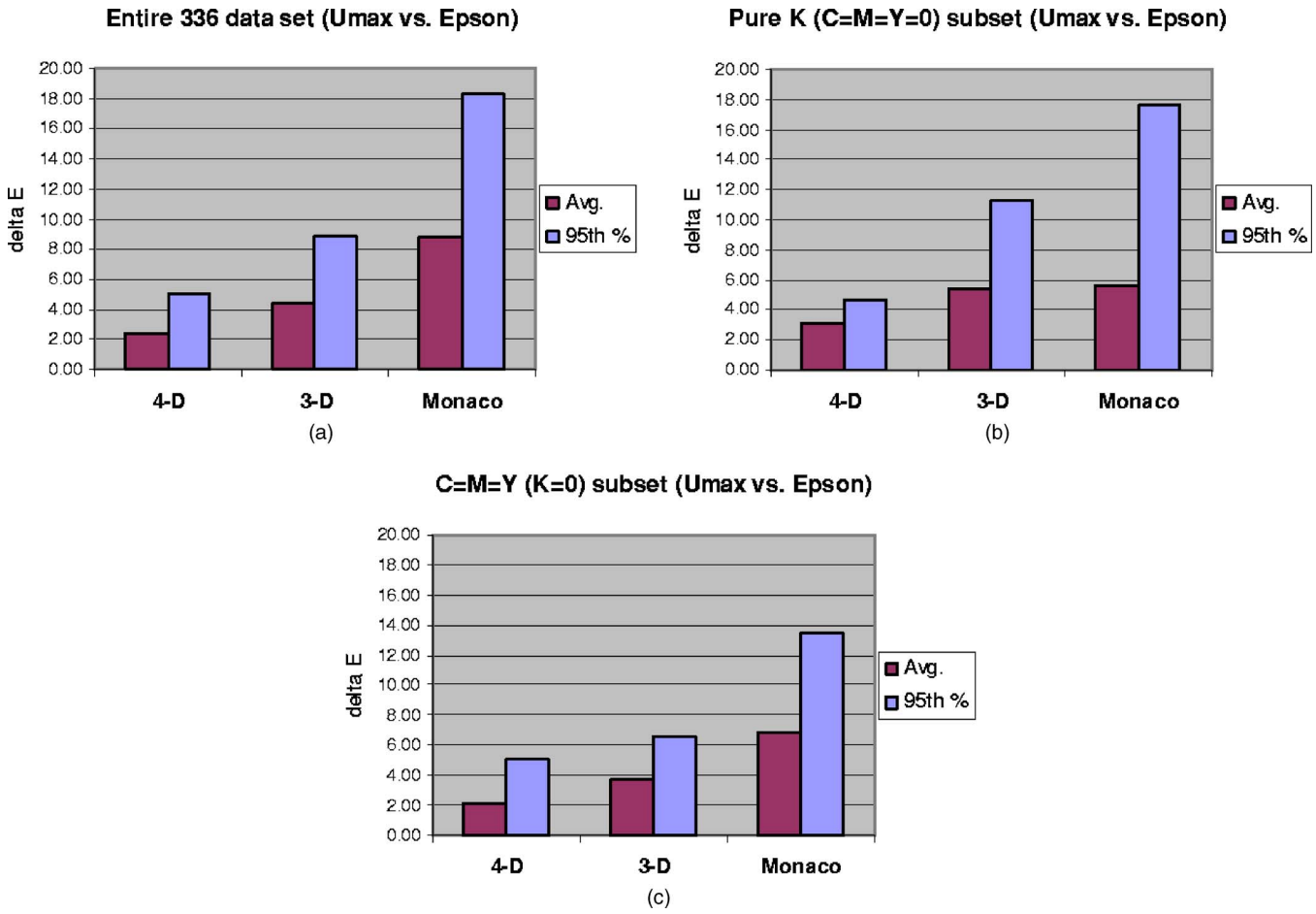

Fig. 15 Robustness of scanner characterization methods across two scanners.

and significantly improved over the 3D and Monaco EZcolor methods, especially for the Umax scanner.

4.4 *Consistency Across Scanners, Media, Halftones*

4.4.1 *The effect of varying scanners*

We performed a test to evaluate each scanner characterization method in terms of consistency achieved across different scanners. This provides a measure of robustness with respect to variations in the capture device. Again, the CMYK336 target was used for the test. Figure 15 shows the results. In general, the 4D approach produces more consistent estimates of CIELAB when different scanners are used.

4.4.2 *The effect of varying substrate and halftone*

Here we report on the impact of varying the substrate and halftone on the accuracy of 4D vs. 3D vs. Monaco EZcolor scanner characterizations. Figure 16 shows the results. We observe that, in both cases, the 4D approach outperforms 3D and Monaco EZcolor. It is also interesting to see that for all characterization methods, the test across different substrates produced smaller errors than the test across different halftones.

5 Conclusion

For color measurement and diagnostics applications that utilize a scanner as a measurement device, a significant improvement in accuracy can be obtained by the judicious combination of target design and additional dimensions in the calibration transform that help resolve scanner metamerism. For the common case of CMYK prints, the method proposed in this paper utilizes a fourth dimension corresponding to the black (K) colorant combined with a pure K target and offers a marked improvement in accuracy over conventional "3D" characterization techniques. Experimental results demonstrate that the proposed 4D characterization method is also more robust with respect to variations in scanners, substrates, and halftones.

Acknowledgment

The authors would like to thank the anonymous manuscript reviewers for their comments and suggestions, which have significantly improved the presentation in the paper.

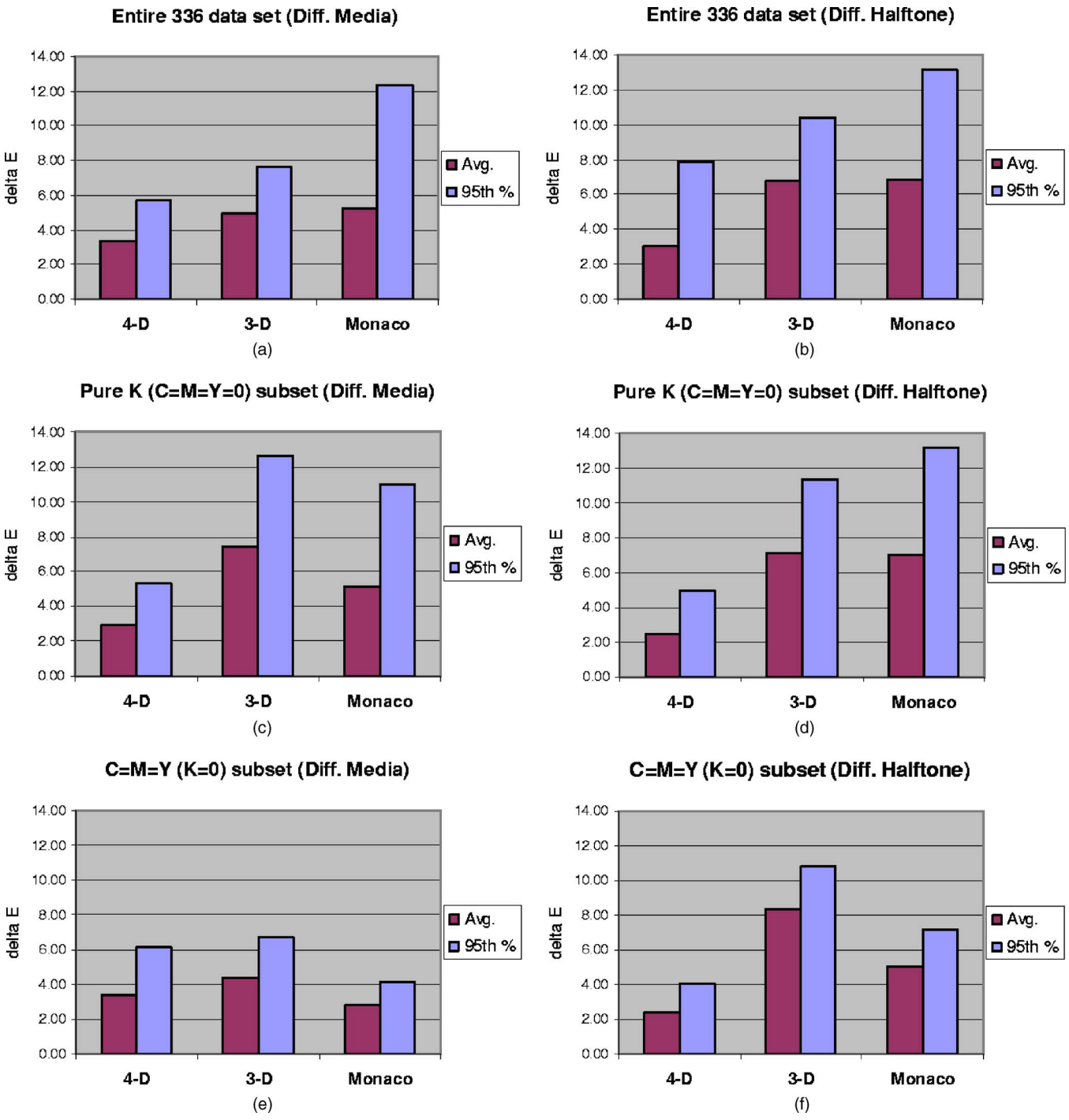

Fig. 16 Impact of using different substrates (left column) and different halftones (right column).

References

1. M. Sampath, R. M. Rockwell, R. D. Rasmussen, A. V. Godambe, E. Jackson, and R. Minhas, "Automated banding defect analysis and repair for document processing systems," US Patent 6,862,414, issued Mar. 1 (2005).
2. M. Sampath, S. J. Nichols, and E. A. Richenderfer, "Systems and methods for automated image quality based diagnostics and remediation of document processing systems," US Patent 6,665,425, issued Dec. 16 (2003).
3. H. Mizes and D. A. Viassolo, "Method of adjusting print uniformity," US Patent 6,819,352, issued Nov. 16 (2004).
4. P. G. Roetling, J. E. Stinehour, and M. S. Maltz, "Color characterization of a scanner," in *Proc. IS&T 7th Int. Cong. on Non-impact Printing*, pp. 443–451 (1991).
5. R. E. Burger, "Device independent color scanning," in *Device-Independent Color Imaging and Imaging Systems Integration*, *Proc. SPIE* **1909**, 70–74 (1993).
6. P. G. Engeldrum, "Color scanner design requirements," in *Device-Independent Color Imaging and Imaging Systems Integration*, *Proc. SPIE* **1909**, 75–83 (1993).
7. H. Haneishi, T. Hirao, A. Shimazu, and Y. Miyake, "Colorimetric precision in scanner calibration using matrices," in *Proc. Third IS&T/SID Color Imaging Conference: Color Science, Systems and Applications*, pp. 106–108 (1995).
8. G. Sharma, S. Wang, D. Sidavanahalli, and K. T. Knox, "The impact of UCR on scanner calibration," in *Final Prog. Proc. IS&T's PICS Conf.*, pp. 121–124 (1998).
9. G. Sharma and S. Wang, "Spectrum recovery from colorimetric data

for color reproductions," in *Color Imaging: Device-Independent Color, Color Hardcopy, and Applications VII*, *Proc. SPIE* **4663**, 8–14 (2002).
10. M. Nier and M. E. Courtot, Eds., *Standards for Electronic Imaging Systems*, paper# CR37, SPIE Optical Engineering Press, Bellingham, WA (1991).
11. R. Bala, "Device characterization," *Digital Color Imaging Handbook*, Ch. 5, G. Sharma, Ed., CRC Press, Boca Raton, FL (2003).
12. K. T. Knox, "Integrating cavity effect in scanners," in *Proc. IS&T/OSA Optics & Imaging in the Information Age*, pp. 83–86 (1996).
13. V. Ostromoukhov, R. D. Hersch, C. Peraire, P. Emmel, and I. Amidror, "Two approaches in scanner-printer calibration: colorimetric space-based vs. closed-loop," in *Device-Independent Color Imaging*, *Proc. SPIE* **2170**, 133–142 (1994).
14. R. L. deQueiroz, K. Braun, and R. Loce, "Detecting spatially varying gray component replacement with application in watermarking printed images," *J. Electron. Imaging* **14**(3), 033016 (2005).

Bong-Sun Lee was a senior research engineer at Samsung Techwin Co., Ltd. (formerly Samsung Aerospace Co., Ltd.), Seoul, Korea, from 1992 to 1999, where he worked on embedded system design, color image processing, color reproduction, and color management for a digital still camera system. He received his PhD degree in electrical and computer engineering from Purdue University, West Lafayette, IN, in 2005. His research interests included psychophysics and human visual system, printer halftoning, and printer defect analysis. Since June 2005, he has been employed at Thomson Corporate Research, Burbank, CA, as a research and technical staff member working on color management and calibration for a film post production, digital cinema, and professional- and consumer-level display systems.

Raja Bala received his PhD degree from Purdue University in electrical engineering. Since then he has been employed at Xerox Innovation Group, where he is currently a principal color scientist working on color imaging algorithms and systems. Raja has also served as an adjunct professor in the Electrical Engineering Department at the Rochester Institute of Technology. Raja holds over 80 publications and patents in the field of color imaging. He is a member of IS&T.

Gaurav Sharma received his BE degree in electronics and communication engineering from the Indian Institute of Technology Roorkee (formerly Univ. of Roorkee), India, in 1990; his ME degree in electrical communication engineering from the Indian Institute of Science, Bangalore, India, in 1992; and his MS degree in applied mathematics and PhD degree in electrical and computer engineering from North Carolina State University, Raleigh, in 1995 and 1996, respectively. From Aug. 1992 through Aug. 1996, he was a research assistant at the Center for Advanced Computing and Communications in the ECE Department at NCSU. From Aug. 1996 through Aug. 2003, he was with Xerox Research and Technology, in Webster, NY, initially as a member of research staff and subsequently at the position of principal scientist. Since fall 2003, he has been an associate professor at the University of Rochester in the Department of Electrical and Computer Engineering and in the Department of Biostatistics and Computational Biology. Dr. Sharma's research interests include color science and imaging, multimedia security and watermarking, and genomic signal processing. He is the editor of the *Color Imaging Handbook* published by CRC Press in 2003. He is a member of IS&T, a senior member of the IEEE, and a member of the Sigma Xi, Phi Kappa Phi, Pi Mu Epsilon honor societies. He currently serves as an associate editor for the *Journal of Electronic Imaging*, *IEEE Transactions on Image Processing*, and *IEEE Transactions on Information Forensics and Security*.